Parameters Affecting Low-pH-Mediated Fusion of Liposomes with the Plasma Membrane of Cells Infected with Influenza Virus

Gerrit van Meer,* Jean Davoust, and Kai Simons
European Molecular Biology Laboratory, D-6900 Heidelberg, FRG
Received November 6, 1984

ABSTRACT: Unilamellar liposomes can be fused at low pH with the plasma membrane of cells that express the hemagglutinin glycoprotein of influenza virus on their surface [van Meer, G., & Simons, K. (1983) *J. Cell Biol. 97*, 1365–1374]. Here, we have resolved this fusion process into two kinetically distinct steps. The first and more rapid step converts the bound liposome to a form that can no longer be released by neuraminidase. The second step is the actual membrane fusion as measured by the loss of resonance energy transfer between two liposomal fluorescent phospholipids, *N*-(7-nitro-2,1,3-benzoxadiazol-4-yl)dioleoylphosphatidylethanolamine (*N*-NBD-PE) and *N*-(lissamine rhodamine B sulfonyl)dioleoylphosphatidylethanolamine (*N*-Rh-PE). In contrast to the first step, the rate of the second one was highly dependent on the liposomal lipid composition and the cell type used. The replacement of 50% of the phosphatidylcholine (PC) in egg PC–cholesterol liposomes by unsaturated phosphatidylethanolamine (PE) species increased the rate of fusion at least 2-fold. Of the PE-containing liposomes that were associated with Madin–Darby canine kidney (MDCK) cells after 30 s of fusion, 80% had actually fused with the plasma membrane. Fringe pattern fluorescence photobleaching experiments showed that after fusion a fraction of the cell-associated *N*-Rh-PE diffused laterally in the plasma membrane. Without fusion, the *N*-Rh-PE was completely immobile. Under optimal conditions, the mobile fractions were 65% on MDCK cells and 78% on baby hamster kidney cells. The mobility was acquired simultaneously with the dilution of the fluorescent phospholipids as measured from the loss of resonance energy transfer. The mobile fraction of *N*-Rh-PE on the cell surface can therefore be used as a second independent measure of actual membrane fusion. Finally, we observed that upon fusion up to 80% of the nonexchangeable liposome markers cholesterol [^{14}C]oleate and glycerol tri[^{14}C]oleate became accessible to cellular hydrolases. The results showed that this hydrolysis assay can also be used to monitor the second step of the fusion process.

In recent years, there has been an ongoing effort to develop methods for fusing liposomes with the plasma membrane of living cells (Gregoriadis, 1980). However, although liposomes could be induced to fuse with one another [see Papahadjopoulos et al. (1979) and Struck et al. (1981)] or with isolated intracellular membranes (Schneider et al., 1980; Ekerdt et al., 1981; Bental et al., 1984), liposomes added to cells either adhere or become endocytosed. At the moment, only one method has been shown to result in controlled and efficient fusion of liposomes with the cell plasma membrane. It makes use of the spike glycoprotein of influenza virus as a fusogen (van Meer & Simons, 1983).

The spike glycoproteins of a number of enveloped viruses display fusogenic properties at low pH [for a review, see White et al. (1983)]. These viruses normally enter their host cells by endocytosis. In the acidic endosome compartment, a fusion reaction is triggered between the viral envelope and the endosomal membrane that delivers the nucleocapsid into the cytoplasm. In the method which we use to fuse unilamellar liposomes with the plasma membrane of Madin–Darby canine kidney (MDCK)[1] cells, the cells are first infected with influenza N virus (van Meer & Simons, 1983). When the HA appears on the surface, it is cleaved into its fusogenic HA_1 and HA_2 subunits by trypsin treatment. Unilamellar liposomes containing a ganglioside with a terminal sialic acid are then allowed to bind to HA_1 on the cell surface, and fusion is subsequently induced by a short treatment (1 min) of the cells at low pH.

The aim of the present study was to optimize the liposome–cell fusion process. We analyzed the influence of pH, liposomal lipid composition, liposome size, and cell type (MDCK and BHK cells) on the fusion reaction. We have used four assays, each of which monitored a different aspect of the fusion process. First, we measured the residual binding of radioactively labeled liposomes to the cell surface after a neuraminidase treatment (Matlin et al., 1981; van Meer & Simons, 1983). Second, we monitored the metabolic fate of the nonexchangeable liposome markers cholesterol [^{14}C]oleate (Kamp et al., 1973; Rothman & Dawidowicz, 1975) and glycerol tri[^{14}C]oleate (Zilversmit, 1971). Third, we monitored the resonance energy transfer between two nonexchangeable fluorescent phospholipids, *N*-NBD-PE and *N*-Rh-PE, incorporated in the liposomes (Struck et al., 1981). Finally, we determined the lateral diffusion properties of the nonexchangeable fluorescent phospholipid *N*-Rh-PE, incorporated in the liposomes, by fringe pattern fluorescence photobleaching (Davoust et al., 1982).

Using these assays, two steps in the fusion process could be defined, one due to a change of the mode of binding between the liposome and the plasma membrane and another which led to fusion of the apposed bilayers.

Materials and Methods

Preparation of Liposomes by Octyl β-D-Glucoside Dialysis.

[1] Abbreviations: BHK, baby hamster kidney; BSA, bovine serum albumin; cmc, critical micelle concentration; EDTA, ethylenediaminetetraacetate; G_{D1a}, IV^{3}NeuAcII^{3}NeuAcGgOse$_4$Cer; HA, hemagglutinin; HEPES, *N*-(2-hydroxyethyl)piperazine-*N*′-2-ethanesulfonic acid; HP-TLC, high-performance thin-layer chromatography; MDCK, Madin–Darby canine kidney; *N*-NBD-PE, *N*-(7-nitro-2,1,3-benzoxadiazol-4-yl)dioleoylphosphatidylethanolamine; *N*-Rh-PE, *N*-(lissamine rhodamine B sulfonyl)dioleoylphosphatidylethanolamine; PBS, phosphate-buffered saline, Dulbecco's formulation (containing 1 mM Ca^{2+} and 0.5 mM Mg^{2+}); PC, phosphatidylcholine; DPPC, dipalmitoylphosphatidylcholine; PE, phosphatidylethanolamine; PS, phosphatidylserine; SD, sample standard deviation; MEF, modulated emission of fluorescence.

0006-2960/85/0424-3593$01.50/0

Five hundred nanomoles of egg PC (egg PC liposomes), egg PC/egg PE (1:1 mol/mol; egg PC/egg PE liposomes), or egg PC/soy PE (1:1 mol/mol; egg PC/soy PE liposomes) plus 500 nmol of cholesterol, 50 nmol of ganglioside G_{D1a}, 10 nmol each of *N*-NBD-PE and *N*-Rh-PE, and 5×10^5 cpm of the nonexchangeable marker cholesterol [^{14}C]oleate (~7.5 nmol), glycerol tri[1-^{14}C]oleate (~7 nmol), or di[1-^{14}C]palmitoyl-PC (~3.5 nmol) were mixed from stock solutions in $CHCl_3$/CH_3OH (2:1 v/v). To this mixture was added 3 mg of octyl β-D-glucoside. After the lipids were dried under a stream of N_2 at 37 °C and suspended into 1 mL of PBS (Dulbecco's formulation) without Ca^{2+} or Mg^{2+}, this resulted in an initial octyl β-D-glucoside concentration of 10 mM, i.e., below the cmc of 22 mM (Helenius et al., 1981). After dialysis for 24 h at 4 °C against three changes of 0.4 L of Ca^{2+}- and Mg^{2+}-free PBS, a homogeneous population of 35-nm-diameter "small" liposomes was obtained by centrifugation of the liposome suspension for 60 min at $100000g_{max}$ at 4 °C (van Meer & Simons, 1983), the yield of the liposomes in the supernatant being over 50%. If in the above procedure 9 mg of octyl β-D-glucoside was used, giving an initial concentration of 31 mM, 50–60% could be pelleted by centrifugation for 60 min at $48000g_{max}$ at 4 °C in the SS34 rotor of a Sorvall centrifuge. After resuspension, electron microscopy of liposomes negatively stained with 2% neutral potassium phosphotungstate in water (Helenius et al., 1977) showed unilamellar liposomes with a mean diameter of 200 nm. These were consequently termed "large" liposomes. Liposomes were stored at 4 °C under nitrogen. Experiments performed within 4 days after the preparation gave identical results.

Cells. MDCK cells, strain II [Matlin & Simons, 1983; for nomenclature, see Balcarova-Ständer et al. (1984)], were grown as described before (van Meer & Simons, 1983). For all experiments, the released cells were plated at a density of 8×10^4 cells/cm^2 in 40-mm-diameter plastic dishes. When resonance energy transfer was to be measured, the cells were grown on 13×27 mm^2 glass coverslips; for photobleaching experiments, they were grown on 20×20 mm^2 glass coverslips in 40-mm-diameter petri dishes. After 48 h, the cells had formed a confluent monolayer of 2×10^6 cells per dish and had not yet formed domes.

BHK-21 cells were grown as described by Renkonen et al. (1972). MDCK strain I cells were grown on permeable supports as described by Fuller et al. (1984).

Virus. Influenza N virus (A/chick/Germany/49, Hav2 Neq 1) was obtained from H.-D. Klenk [Institut für Virologie, Universität Giessen, FRG (Klenk et al., 1975)]. Virus stocks were prepared and plaque titrations performed as described previously (Matlin & Simons, 1983). Identical results for the time course of infection, levels of liposome binding/fusion, and the pH dependence of fusion were obtained with the human influenza virus strain X-31 (A/Hong Kong/1968 H3 N2) which was obtained from J. Skehel (National Institute for Medical Research, Mill Hill, U.K.).

Fusion of Liposomes with Virus-Infected Cells. Confluent 2-day-old monolayers of MDCK cells were infected with 20 plaque-forming units of influenza N virus per cell suspended in 0.2 mL of Earle's MEM supplemented with 10 mM HEPES, penicillin, streptomycin, and 0.2% BSA. The virus was allowed to adsorb for 1 h at 37 °C, after which the inoculum was replaced by Earle's MEM supplemented with 10 mM HEPES and 5% fetal calf serum. At 4.5 h after infection with influenza N virus, the cell monolayer was washed with 1 mL of ice-cold "binding medium", which consisted of Earle's MEM without bicarbonate supplemented with 10 mM HEPES and 0.2% BSA, pH 7.4, and cooled on a metal plate on ice with 1 mL of binding medium. Because the HA protein of influenza N virus is not proteolytically cleaved into its HA_1 and HA_2 subunits in MDCK cells, which is necessary for its fusogenic activity, cleavage was brought about by the addition of trypsin (Matlin & Simons, 1983). The cells were washed twice with 1 mL of ice-cold PBS, and 1 mL of an ice-cold solution of L-1-(tosylamido)-2-phenylethyl chloromethyl ketone treated trypsin (100 μg/mL PBS) was added. After gentle shaking on ice for 15 min, 100 μL of soybean trypsin inhibitor solution (1 mg/mL PBS) was added and shaking continued for 5 min. The dishes were then washed with 1 mL of a soybean trypsin inhibitor solution of 100 μg/mL in PBS. Subsequently, 200 μL of a suspension of lipid vesicles in binding medium containing 2 nmol of phospholipid was spread over the cell monolayer, if this had been grown on plastic dishes. To dishes with coverslips was added 5 nmol of vesicle phospholipid in 500 μL. The dishes were gently shaken on ice, and after 30 min, the vesicle suspension was aspirated, leaving the bound vesicles on the cell surface. Five milliliters of warm (37 °C) fusion medium, consisting of Earle's MEM without bicarbonate supplemented with 20 mM succinate and 0.2% BSA of a defined pH between 4.9 and 5.7, was then added to the cells, and the dish was placed on the surface of a 37 °C water bath. After varying time intervals, the dish was returned to the ice-cold metal plate and washed twice with ice-cold binding medium. Subsequently, cells on coverslips were used for fluorescence measurements and subsequent quantitation of radioactivity as described below. The cell monolayers on plastic were used for quantitative analyses.

Quantitation of Neuraminidase-Resistant Binding. To quantitate the amount of cell-associated liposomes which were resistant against release by neuraminidase, the neuraminidase-sensitive liposomes had to be removed from the cell surface. For this purpose, the cell monolayer was incubated for 30 s at 37 °C and pH 7.4. This is long enough to allow the viral neuraminidase present at the cell surface to remove any neuraminidase-sensitive liposomes (van Meer & Simons, 1983). Subsequent treatment with *Clostridium perfringens* neuraminidase (2 mg/0.5 mL of PBS; 30 min, 0 °C) did not release additional liposomes from the cells. The pH 7.4 treatment was omitted if the liposomes had been fused to the cells for 30 s or longer at 37 °C. The cells were then scraped from the dish, transferred to a vial filled with a scintillation fluid containing Triton X-100 (Rotiszint, Carl Roth KG., Karlsruhe, FRG), and counted for radioactivity in a Mark III liquid scintillation spectrometer (Searle Analytic, Des Plaines, IL). When cell monolayers on coverslips were used, the resonance energy transfer was measured as described below, and subsequently, the coverslip was transferred directly into the scintillation vial.

Fluorescence Measurements. Steady-state emission spectra were obtained by using an MPF-44A fluorescence spectrophotometer (Perkin-Elmer, Norwalk, CT). The apparatus was used in the ratio mode, and the excitation and emission band slits were set to obtain a resolution of 10 nm. All samples were excited at 470 nm, and the 480–650-nm fluorescence emission spectrum was recorded at a rate of 120 nm/min. A long-wavelength pass filter with a cutoff at 475 nm (type GG475) was placed in the outgoing pathway, and crossed polarizers were installed to minimize the background signal due to scattered light.

These filters were necessary to allow the recording of emission spectra from an intact monolayer of cells. For this purpose, a monolayer of cells was grown on 13×27 mm^2 glass

coverslips, the cells were infected with virus, and lipid vesicles were fused to them as described above. Subsequently, the coverslip was taken from the petri dish, rinsed in PBS, and placed in a vertical position diagonally across a 10 × 10 mm^2 fluorescence cuvette, filled with PBS. From the two possible diagonal positions, that position was chosen in which reflected light from the incoming beam would be reflected away from the outgoing pathway. The fluorescence emission spectrum was recorded, and since the beam of the excitation light only illuminated a discrete spot on the lower half of the coverslip, a second independent spectrum could be recorded from the same coverslip by simply turning it upside down in the cuvette. The background of a cell monolayer on a coverslip in the absence of fluorescent lipids and the background to signal ratio were as low as those reported for measurements on cells scraped from a dish and resuspended into the cuvette (van Meer & Simons, 1983). The present method has two advantages over the latter one: possible cell damage due to scraping and resuspending is prevented, and 30× less cells are needed for a single measurement.

The kinetics of fusion can be recorded continuously by performing the fusion reaction in the cuvette (Eidelman et al., 1984). This method was applied to a monolayer of MDCK cells on a coverslip. Although fusion was indeed observed as a time-dependent increase in the fluorescence emission at 535 nm, the rate of fusion could not be accurately determined by this method because considerable loss of total fluorescence from the coverslip occurred on the time scale of the experiment. This is due to the fact that, during the first 10 s of fusion, about 50% of the cell-associated liposomes are released from the cell monolayer (van Meer & Simons, 1983) and diluted into the cuvette.

Calculations of Resonance Energy Transfer. Fluorescence energy transfer assays according to Struck et al. (1981) were carried out as described previously (van Meer & Simons, 1983). The efficiency of energy transfer in the original lipid vesicles (E) was calculated from the relative intensity of the N-NBD-PE emission at 530 nm (F) and the total emission of the sample after energy transfer was abolished by the addition of Triton X-100 (with the necessary corrections for sample dilution and lower quantum yield: ×1.39; F_0), the relationship between these parameters being $E = 1 - F/F_0$ (Fung & Stryer, 1978; Struck et al., 1981). Identical results were obtained when the efficiency of energy transfer was calculated directly from the relative intensities of the N-NBD-PE emission at 530 nm and the N-Rh-PE emission at 590 nm with the necessary corrections: the N-Rh-PE emission at 590 nm had to be corrected for the N-NBD-PE emission at 590 nm (51% ± 3% of N-NBD-PE emission at 530 nm, mean followed by SD from seven experiments), and the N-NBD-PE emission at 530 nm had to be corrected for its lower fluorescence emission amplitude at this wavelength compared to that of N-Rh-PE at 590 nm. This turned out to be 60% ± 5% (mean followed by SD from seven experiments).

The resonance energy transfer in the original vesicles was different in the two vesicle preparations: for the large vesicles, it was 76% ± 1% (n = 6) and for the small vesicles 90% ± 1% (n = 5). The concentration of N-NBD-PE and N-Rh-PE in the $CHCl_3/CH_3OH$ stock solutions was determined according to Rouser et al. (1970). After all incubations, the fluorescent group was still present in the original molecule as controlled by two-dimensional HP-TLC.

Analysis of the commercially obtained N-Rh-PE by two-dimensional HP-TLC (Renkonen et al., 1972; van Meer & Simons, 1982) showed that one commercially obtained preparation contained a second fluorescent isomer of N-Rh-PE which displayed a pH-dependent quantum yield with R_f values of 0.5 and 0.7 in the alkaline and acid direction, respectively, as compared to 0.8 and 0.9 for the pH-independent isomer. Only preparations containing over 90% of the pH-independent isomer were used in this study. Fluorescent degradation products of N-Rh-PE were never observed before or after fusion.

Fluorescence Photobleaching Experiments. Measurements of fluorescence recovery after photobleaching were performed in an inverted Zeiss IM35 microscope equipped with a 63× Plan Neofluar objective, epifluorescence filters, and a temperature-controlled stage. A field of 60-μm diameter was illuminated with two superimposed coherent laser beams (λ = 514 nm) that define a fringe pattern. After the production of a striped pattern of fluorescence by a photobleaching pulse, the amplitude of the periodical fluorescent concentration profile was converted into a modulated emission of fluorescence by using the oscillating pattern technique with a vibration frequency of 3 kHz (Davoust et al., 1982). The fluorescent light was collected from the sample area of interest and detected with a Hamamatsu R647-01 photomultiplier. The modulated emission of fluorescence (MEF) was measured from the total fluorescence signal by using a lock-in amplifier. Simultaneously, the average fluorescence signal level was determined after low-pass filtering and direct-current amplification. The noise was filtered with a tunable time constant set in our experiments to 300 ms (12 dB). Further experimental details about this instrument will be given elsewhere (J. Davoust et al., unpublished results). Related pattern fluorescence photobleaching methods have been used previously to estimate lateral diffusion coefficients (Smith & McConnell, 1978; Smith et al., 1979; Lanni & Ware, 1984; Miles et al., 1984).

A 20 × 20 mm^2 coverslip with a monolayer of cells to which liposomes had been fused with N-Rh-PE as a fluorescent probe was mounted on the stage of the microscope immersed in binding medium, and the temperature was kept at 5 °C. A fringe pattern with a repetitive distance (l) of 4–10 μm was applied to the cells, and a short bleaching pulse was delivered (less than 100 ms with an intensity of 1000 W/cm^2) by which less than 20% of the cell-associated fluorophores were bleached. Subsequently, the fluorescence recovery in the bleached lines and the fluorescence loss from the nonbleached lines were recorded as a loss in MEF signal, and the average fluorescence signal level was determined at the same time. Always as a control, the same signals were recorded before the onset of the bleaching pulse (Davoust et al., 1982). During the monitoring times (before as well as after the bleaching pulse), the light level was attenuated to less than 1 W/cm^2, and no appreciable additional bleaching of the fluorophores was observed.

Analysis of Cholesterol [^{14}C]Oleate Hydrolysis. After the fusion of the liposomes with the cells, the cell monolayers were incubated for varying lengths of time at 0 and 37 °C, washed once with ice-cold binding medium, and scraped from the plastic with a rubber policeman into 3 mL of ice-cold binding medium. The cells were pelleted at $200g_{max}$ for 5 min at 4 °C, and the lipids were extracted according to the method of Bligh & Dyer (1959). The $CHCl_3$ phase from the extraction was dried under N_2 at 37 °C, and the lipids were spotted onto precoated silica gel HP-TLC plates (Merck, Darmstadt, FRG). The plates were developed in a solvent system consisting of hexane/diethyl ether/acetic acid (90:10:1 v/v). The R_f values for cholesterol oleate, triglyceride, free fatty acid, cholesterol, diglyceride, and (lyso)phospholipid were determined with radioactive standards. A clean separation of these

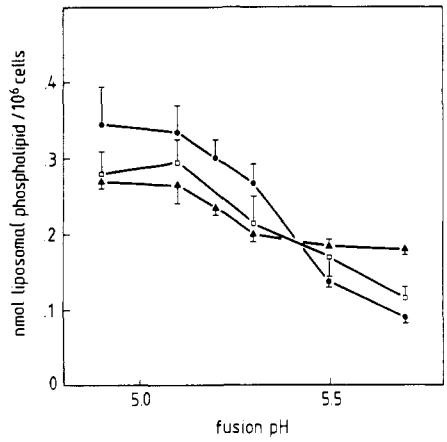

FIGURE 1: Induction of neuraminidase-resistant liposome–cell association by low pH. A monolayer of MDCK cells on 13 × 27 mm² coverslips, infected with influenza N virus, was treated with trypsin as described under Materials and Methods. Liposomes were bound to the cells, and fusion medium of a defined pH was added for 60 s at 37 °C. Neuraminidase-sensitive liposomes were removed during the incubation at 37 °C by the viral neuraminidase at the cell surface. Radioactivity on the coverslips was quantitated as described under Materials and Methods. Each point represents the mean of four measurements; the bar indicates the SD. (□) Small liposomes of egg PC/cholesterol/G_{D1a}/*N*-NBD-PE/*N*-Rh-PE (1:1:0.1:0.02:0.02 mol/mol, egg PC liposomes); (●) large liposomes of egg PC/egg PE/cholesterol/G_{D1a}/*N*-NBD-PE/*N*-Rh-PE (0.5:0.5:1:0.1:0.02:0.02 mol/mol, egg PC/egg PE liposomes); (▲) large liposomes of egg PC/soy PE/cholesterol/G_{D1a}/*N*-NBD-PE/*N*-Rh-PE (0.5:0.5:1:0.1:0.02:0.02 mol/mol, egg PC/soy PE liposomes). All liposomes contained [^{14}C]DPPC as a nonexchangeable marker.

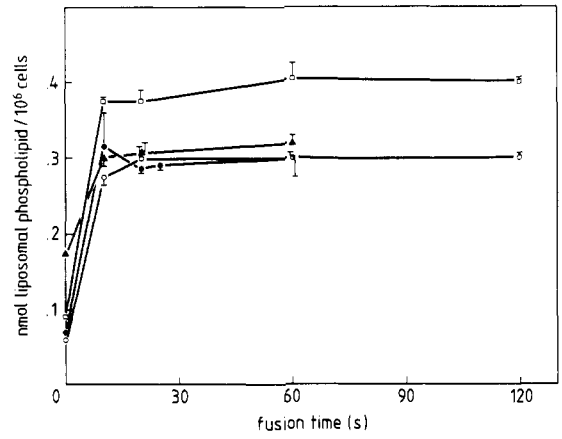

FIGURE 2: Time course of the induction of neuraminidase-resistant liposome–cell association by pH 5.1. The experiments were performed as described in Figure 1. Fusion was performed at pH 5.1 for different time periods. In each case, the cells were warmed to 37 °C at pH 7.4 for an additional 30 s to allow the viral neuraminidase to remove any remaining neuraminidase-sensitive liposomes. Each point represents the mean of four measurements; the bar indicates the SD. (□) Small egg PC liposomes; (○) small egg PC/egg PE liposomes; (●) large egg PC/egg PE liposomes; (▲) large egg PC/soy PE liposomes.

lipid classes was obtained [see Jagannatha & Sastry (1981)]. The lipid spots were visualized by staining with iodine vapor, marked, and left to destain. The spots were scraped into scintillation vials and counted for radioactivity as described above.

Sources of Reagents. *N*-NBD-PE and *N*-Rh-PE were obtained from Avanti Polar Lipids, Inc. (Birmingham, AL). Egg PC, egg PE, soy PE, bovine brain PS, *Clostridium perfringens* neuraminidase (1 IU/mg of protein), cholesterol, and buffer salts were obtained from Sigma Chemical Co. (St. Louis, MO). G_{D1a} and saturated PE, under the designation "egg PE", were from Supelco, Inc. (Bellefonte, PA). Cholesterol [1-^{14}C]oleate (50.8 Ci/mol), glycerol tri[1-^{14}C]oleate (55.5 Ci/mol), and di[1-^{14}C]palmitoyl-PC (112 Ci/mol) were purchased from Amersham International (Amersham, U.K.) Octyl β-D-glucoside was from Calbiochem-Behring Corp. (La Jolla, CA). Trypsin–L-1-(tosylamido)-2-phenylethyl chloromethyl ketone and soybean trypsin inhibitor were obtained from Millipore Corp. (Freehold, NJ). Fetal calf serum was from KC Biologicals (Lenexa, KS). Chemicals and solvents were of analytical grade and obtained from Merck (Darmstadt, FRG).

RESULTS

Neuraminidase-Resistant Liposome–Cell Association. A monolayer of MDCK cells was infected with influenza N virus and treated with trypsin 4.5 h after infection, and liposomes were bound to the cells at 0 °C, as described under Materials and Methods. The liposomes bind to the HA on the cell surface by means of the terminal sialic acid residue of the ganglioside G_{D1a}. At 37 °C, this residue is removed efficiently by the viral neuraminidase present on the plasma membrane of infected cells, resulting in liposome release. However, when the cells are warmed to 37 °C in a medium of low pH, the liposome–cell association becomes neuraminidase resistant (van Meer & Simons, 1983). The pH dependence of this process is shown in Figure 1 and the time dependence in Figure 2. Neuraminidase resistance is induced by pHs lower than 5.5 and reaches a maximum at pH 5.1. The reaction is virtually complete by 10 s, which is the shortest time point that could be accurately studied. Liposomes of different lipid composition showed essentially identical behavior except for the fact that the nonspecific binding was higher in soy PE containing liposomes, 0.17 ± 0.03 nmol of phospholipid/10^6 cells (n = 3) as compared to 0.08 ± 0.01 nmol of phospholipid/10^6 cells (n = 6) for egg PE containing liposomes. In addition, the level of low-pH-induced neuraminidase-resistant binding was slightly different for the various types of liposomes: expressed as nanomoles of phospholipid per 10^6 cells, the levels were 0.33 ± 0.05 (n = 5) for small egg PC liposomes, 0.25 ± 0.03 (n = 2) for large egg PC/saturated PE liposomes, 0.28 ± 0.03 (n = 2) for small egg PC/egg PE liposomes, 0.30 ± 0.05 (n = 4) for large egg PC/egg PE liposomes, and 0.25 ± 0.03 (n = 5) for large egg PC/soy PE liposomes. A typical experiment is shown in Figure 2. If the experiments were performed with cells on plastic instead of cells on coverslips (see Materials and Methods), the levels of binding were 40% less.

Dependence of Fusion on Lipid Composition. The fraction of the cell-associated liposomes that has actually fused to the plasma membrane after the low-pH incubation can be accurately determined from the loss of resonance energy transfer between *N*-NBD-PE and *N*-Rh-PE (Struck et al., 1981) in the cell monolayer compared to the starting liposomes. For liposomes with a matrix of egg PC/cholesterol, the loss of resonance energy transfer after a 60-s incubation at 37 °C in a medium of pH 5.3 was found to be 45% (van Meer & Simons, 1983). Here, we find that replacement of 50% of the egg PC by egg PE or soy PE induced a steep pH dependence (Figure 3). A sharp increase in the loss of resonance energy transfer in the cell-associated liposomes was observed between pH 5.5 and 5.2. Just as striking was the influence of PE on the fusion efficiency. At pH <5.2, over 80% of the cell-associated PE-containing liposomes had fused with the plasma membrane. The time for half-maximal fusion as monitored by the loss of resonance energy transfer was 60–120 s for egg PC liposomes and approximately 10 s for egg PC/egg PE liposomes (Figure 4).

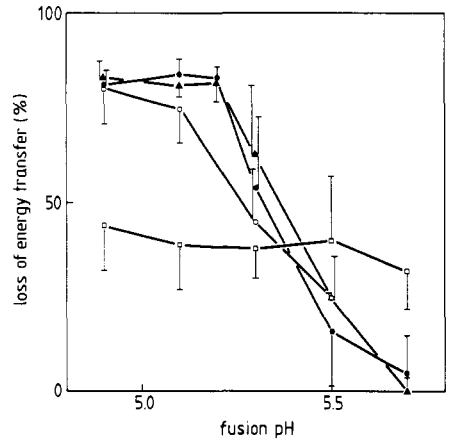

FIGURE 3: Induction of loss of resonance energy transfer between *N*-NBD-PE and *N*-Rh-PE by low pH. Liposomes were fused to virus-infected MDCK cells as described in Figure 1. After the fusion, the coverslip with the cell monolayer was transferred into a fluorescence cuvette filled with PBS. The fluorescence emission spectrum was recorded (λ_{exc} = 470 nm), and the resonance energy transfer was calculated as described under Materials and Methods. Each point represents the loss of energy transfer as the percent of the energy transfer in the original vesicles and is the mean of 8–12 measurements in 2–3 independent experiments. The bar indicates the SD (n = 8–12). The total cell-associated radioactivity is plotted for each pH in Figure 1. (□) Small egg PC liposomes; (○) small egg PC/egg PE liposomes; (●) large egg PC/egg PE liposomes; (▲) large egg PC/soy PE liposomes.

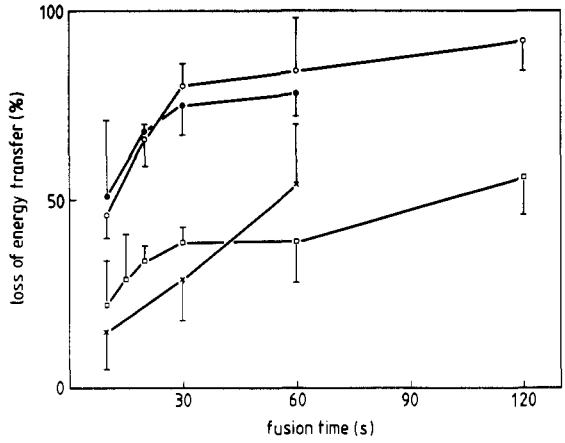

FIGURE 4: Time course of the loss of resonance energy transfer between *N*-NBD-PE and *N*-Rh-PE at pH 5.1 in MDCK cells. Liposomes were bound and fused to virus-infected MDCK cells as in Figure 1. The loss of energy transfer was determined as described in Figure 3. The data points are the mean of 8–12 measurements in 2–3 independent experiments. The bar indicates the SD (n = 8–12). The total cell-associated radioactivity is plotted for each time point in Figure 2. (□) Small egg PC liposomes; (○) small egg PC/egg PE liposomes; (●) large egg PC/egg PE liposomes; (×) large egg PC/saturated PE liposomes.

The fatty acyl composition of PE was an important parameter in fusion. The egg PE used in these experiments has a relatively unsaturated fatty acyl composition: 46% saturated, 17% monounsaturated, 10% 2-fold unsaturated, and 25% 4–6-fold unsaturated fatty acyl chains (Holub & Kuksis, 1969). For soy PE, these numbers are 30% saturated, 9% monounsaturated, 57% 2-fold unsaturated, and 4% 3-fold unsaturated (Crawford & Plattner, 1984). Liposomes prepared with a PE species having 80% saturated and 20% monounsaturated fatty acyl chains (Supelco, Bellefonte, PA; product specification) did not promote fusion compared to the more unsaturated PE's (Figure 4). To test whether peroxidation of the egg PE was involved in its stimulatory effect on fusion, freshly obtained egg PE was artificially peroxidized.

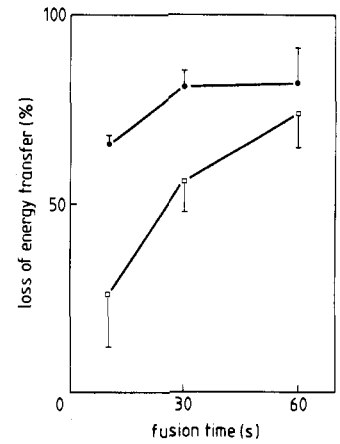

FIGURE 5: Time course of the loss of resonance energy transfer between *N*-NBD-PE and *N*-Rh-PE at pH 5.1 in BHK cells. A monolayer of BHK cells on 13 × 27 mm^2 coverslips was infected with influenza N virus for 4.5 h, and liposomes were bound and fused to the cells as described before. The data points are the mean of four measurements. The bar indicates the SD (n = 4). (□) Small egg PC liposomes; (●) large egg PC/egg PE liposomes.

The egg PE was dried and left under a stream of oxygen for 1 h at 37 °C, by which the oxidation index A_{233nm}/A_{215nm} (Klein, 1970) was changed from 0.28 to 0.50 (as opposed to <0.10 for saturated egg PE or fresh egg PC). Egg PC/egg PE liposomes prepared from the peroxidized PE's had the same rate of fusion as liposomes made from unperoxidized PE (not shown). Thus, the stimulatory effect of PE is due both to the head group and to the unsaturation of the fatty acids.

In addition to PE, PS was also tested for stimulation of fusion. When liposomes with the composition PC/PS/cholesterol (1:1:2 v/v) were bound to and fused with MDCK cells, the rate of loss of energy transfer was similar to that of egg PC liposomes. The total amount of cell-associated liposomes and thereby the total amount of fused lipids were 1.5-fold higher for the PS-containing liposomes. However, the nonspecific binding of PS-containing liposomes, measured as the amount of cell-associated liposomes after 1 min at 37 °C in pH 7.4, was 5-fold higher than for egg PC liposomes. Thus, the higher total level of fusion of PS-containing liposomes appears to be a consequence of higher levels of nonspecific binding rather than more efficient fusion.

The differences in liposome size, 35 as opposed to 200 nm in diameter, had no influence on the rate or the extent of fusion (Figures 2–4).

The fusion of liposomes was also influenced by the recipient plasma membrane. MDCK cells, being polarized cells of epithelial origin, have a highly specialized plasma membrane organization. The liposome–cell fusion was also tested on nonpolarized BHK cells. A time course of the loss of energy transfer is shown in Figure 5 for egg PC and egg PC/egg PE liposomes. The fusion with the plasma membrane of BHK cells was faster than with that of MDCK cells. Also with BHK cells, the replacement of 50% of the egg PC by egg PE resulted in a highly enhanced fusion rate. The pH dependence of the fusion was identical with that for MDCK cells (results not shown).

Identical results were obtained when MDCK cells were infected with X-31 virus, a human influenza A virus strain, instead of influenza N virus. Not only the pH dependence of liposome fusion but also the time course of viral infection and the level of liposome–cell association were exactly the same (results not shown). The latter observation is surprising since the influenza virus receptor used in these studies is G_{D1a} with a NeuAcα2→3Gal linkage and X-31 wild-type virus has been

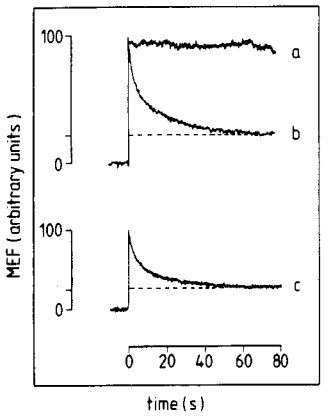

FIGURE 6: Modulated emission of fluorescence (MEF) curves as a function of time. A monolayer of MDCK or BHK cells was grown on 20 × 20 mm² coverslips, infected with influenza N virus, and treated with trypsin at 4.5 h after infection. Liposomes containing 1 mol % *N*-Rh-PE were bound to the cells and fused at pH 5.1 (b and c) and at pH 7.4 (a) for 60 s at 37 °C. The coverslip was then mounted onto the microscope stage at 5 °C, and at $t = 0$, a bleaching pulse was delivered for 100 ms. The fluorescence redistribution was monitored as a function of time as the decrease of contrast between the bleached lines and unbleached lines (MEF) as described under Materials and Methods. The repetitive distance (I) used in the fringe pattern was 4.4 μm for MDCK cells and 8.5 μm for BHK cells. The dashed lines show the extrapolation of the plateau reached to $t = 0$ and are characteristic of an immobile component. The decaying fraction of curves b and c corresponds to the mobile component. The values for the mobile fraction (f_m) and the average half-decay time constant ($t_{1/2}$) are summarized in Table I. (a) Large egg PC/egg PE liposomes; BHK cells, unfused; (b) large egg PC/egg PE liposomes; BHK cells, fused at pH 5.1; (c) large egg PC/egg PE liposomes; MDCK cells, fused at pH 5.1.

reported (Rogers et al., 1983) to have a strict specificity for NeuAcα2→6Gal linkages.

Lateral Diffusion of a Liposome Marker in the Plasma Membrane after Fusion. The lateral mobility of the liposomal fluorescent phospholipid *N*-Rh-PE on the cell surface was monitored with the fringe pattern version of the fluorescence photobleaching technique (Davoust et al., 1982) combined with a fluorescence microscope, as described under Materials and Methods. The diameter of the illuminated field, 60 μm, encompassed up to three whole cells. A large interfringe distance of either 4.4 μm (MDCK cells) or 8.5 μm (BHK cells) was set, so that the diffusion within individual liposomes could not be detected. Under these conditions, the instrument monitored the average fraction of the cell-associated *N*-Rh-PE that diffused freely in the plasma membrane. Since *N*-Rh-PE is nonexchangeable under the conditions used [cf. Struck et al. (1981)], the mobile fraction of the cell-associated *N*-Rh-PE originated from the liposomes that have fused with the plasma membrane.

Liposomes of varying lipid compositions with 1 mol % *N*-Rh-PE were bound to a monolayer of cells and incubated at 37 °C and pH 5.1 for different lengths of time. A striped pattern of fluorescence was subsequently produced on the cell monolayer by a short bleaching pulse, and the contrast of the pattern, converted into a modulated emission of fluorescence (MEF) value, was monitored in time as described under Materials and Methods. Typical curves are shown in Figure 6. When fluorescent liposomes with a matrix of egg PC/cholesterol were bound to the cells but not fused, the MEF remained essentially constant after bleaching (curve a). The same plateau was found for an immobilized test sample composed of a layer of fluorescent proteins (BSA) fixed on a polylysine-coated coverslip (data not shown). When egg PC/egg PE/cholesterol liposomes were fused at low pH for 60 s with either BHK cells (curve b) or MDCK cells (curve c), the MEF decreased until it reached a plateau characteristic of an immobile fraction. This plateau was not found in test samples composed of fluorescent BSA freely diffusing in water/glycerol mixtures (Davoust et al., 1982). The amplitude of the decaying component corresponds to the fraction of *N*-Rh-PE incorporated into the cellular plasma membrane since these fluorescent molecules are now able to move over micrometer distances.

Table I: Diffusion of *N*-Rh-PE on the Surface of MDCK and BHK Cells at 5 °C after Fusion[a]

	fusion time (s)	f_m (%)[b]	$t_{1/2}$ (s)[c]	n
MCDK cells				
egg PC/cholesterol	15	19 ± 7		10
(1:1 mol/mol)	120	20 ± 5		8
egg PC/egg PE/cholesterol	10	58 ± 8	5.8 ± 1.1	11
(1:1:2 mol/mol)	60	65 ± 6	4.7 ± 1.0	14
BHK cells				
egg PC/cholesterol	10	<10		7
(1:1 mol/mol)	60	46 ± 5	6.5 ± 2.0	6
egg PC/egg PE/cholesterol	10	58 ± 6	6.5 ± 2.0	6
(1:1:2 mol/mol)	60	78 ± 9	7.3 ± 2.8	14

[a] Liposomes containing *N*-Rh-PE as a fluorescent marker were fused with the plasma membrane of MDCK or BHK cells at pH 5.1 and 37 °C for the indicated periods of time. Measurements were performed as described in the legend to Figure 6 and under Materials and Methods. [b] f_m represents the average fraction of the cell-associated fluorescence that is present as a mobile component, calculated from the MEF curves (Figure 6). It is followed by the population standard deviation from n measurements performed at different locations on one or more coverslips. It is noteworthy that each individual measurement already represents the average of the plasma membranes of one to three cells present in the 60-μm-diameter field studied, as opposed to the spot photobleaching technique which gives more local information. [c] The values of $t_{1/2}$ correspond to the average half-decay time constant of the mobile component followed by its standard deviation. The repetitive distance used in the fringe pattern was 4.4 μm on MDCK cells and 8.5 μm on BHK cells.

As an index of fusion, the fraction of diffusible *N*-Rh-PE was now measured as a function of the liposomal lipid composition and as a function of the incubation time at pH 5.1. Table I summarizes the average mobile fraction after fusion with MDCK cells or BHK cells. For both cell lines, the amplitude of the mobile fraction was highly dependent on the type of liposome used: egg PC/egg PE liposomes readily fused, resulting in a mobile fraction of 65–78%, while much lower fusion efficiencies were displayed by egg PC liposomes. The results in Table I also indicate a higher fusion rate for BHK cells as compared to MDCK cells. Thus, fusion as measured by lateral diffusion was influenced by the same parameters as fusion measured by loss of resonance energy transfer.

The average lateral diffusion coefficient (D) of *N*-Rh-PE in the cellular plasma membrane can be calculated from the half-decay time constant ($t_{1/2}$) of the MEF curves (Figure 6) according to the formula $D = (I^2 \ln 2)/(4\pi^2 t_{1/2})$. The $t_{1/2}$ was determined whenever the mobile fraction exceeded one-third of the total MEF. The resulting average lateral diffusion coefficients were $(0.69 \pm 0.16) \times 10^{-9}$ cm² s⁻¹ on MDCK cells at 5 °C and $(2.1 \pm 0.7) \times 10^{-9}$ cm² s⁻¹ on BHK cells at 5 °C. However, this calculation assumed that the decaying components of the MEF curves are strictly monoexponential, which was not the case. With both MDCK and BHK cells, the MEF curves deviated significantly from the monoexponential curve which was found for proteins in solution (Davoust et al., 1982) and for *N*-Rh-PE incorporated into oriented lipid multilayers (data not shown). Since one cannot approximate the disposition of the plasma membrane of either MDCK cells or BHK cells with that of an infinite and homogeneously labeled planar

surface, the apparent lateral diffusion coefficients calculated above represent an underestimate of the local lateral diffusion coefficient. In this case, not only the viscous drag of *N*-Rh-PE plays a role but also the folding due to the microvilli and the effect of cell margins account for the nonexponential decay of the MEF and for the apparently slow lateral diffusion coefficients (J. Davoust et al., unpublished results). In contrast, the immobile fraction was characterized by a time constant that is at least 1 order of magnitude above the $t_{1/2}$ of the mobile fraction, giving an upper limit of 5×10^{-11} cm^2 s^{-1} for the diffusion coefficient on this distance scale (4–8 μm) for the *N*-Rh-PE which was present in cell-associated liposomes that had not fused with the plasma membrane.

Cholesterol [^{14}C]Oleate Hydrolysis after Fusion. Quantitation of cell-associated liposomes after the fusion step gave different results when cholesterol [^{14}C]oleate was used as a lipid marker instead of [^{14}C]DPPC. At pHs of 5.5 and below, the levels of cholesterol [^{14}C]oleate found in the cells decreased in contrast to increasing amounts of [^{14}C]DPPC (Figure 1). Apparently, the radioactivity of the former lipid is lost from the cells after low-pH incubations. Since cholesterol [^{14}C]-oleate does not spontaneously exchange between membranes (Kamp et al., 1973; Rothman & Dawidowicz, 1975), the loss would most naturally be explained by hydrolysis of the cholesterol [^{14}C]oleate and subsequent loss of the liberated [^{14}C]oleic acid into the medium. Loss into binding medium was higher than into PBS. The reason for this would be that in the former case the [^{14}C]oleic acid is able to exchange with free fatty acids bound to the BSA, present in that medium.

To quantitate hydrolysis, egg PC/soy PE liposomes containing cholesterol [^{14}C]oleate were fused to MDCK cells for 60 s at pH 5.1. After an additional incubation of 30 min in binding medium on ice, the lipids were extracted separately from the cells and from the binding medium and were analyzed for radioactivity as described under Materials and Methods. Of the total ^{14}C radioactivity, only 45% ± 5% (n = 4) was found associated with the cells, and of this, only 50% ± 2% (n = 4) was localized in the cholesterol ester spot. The remainder was found in free fatty acids [33% ± 2% (n = 4)] and phospholipids [17% ± 2% (n = 4)]. In contrast, 89% ± 1% (n = 4) of the radioactivity that had been released into the medium was present as oleic acid. This implies that 76% of the cell-associated cholesterol [^{14}C]oleate had been hydrolyzed and that two-thirds of the resulting [^{14}C]oleic acid had partitioned into the binding medium. Also, when liposome binding was followed by an incubation of 60 s at 37 °C in medium of pH 7.4 instead of pH 5.1, a significant amount of liposome radioactivity remained cell associated due to the high nonspecific binding of egg PC/soy PE liposomes (Figures 1 and 2). In this case, however, no radioactivity was found in the binding medium, and of the cell-associated radioactivity, 92% ± 1% (n = 4) was found as intact cholesterol [^{14}C]oleate. Hydrolysis was therefore dependent on the low-pH treatment (cf. Figure 1).

With [^{14}C]DPPC, more than 95% of the total radioactivity was always found as intact PC, and no radioactivity was lost into the binding medium. It could thus be used as a nonhydrolyzable marker to measure cell association. In all subsequent experiments, parallel incubations were performed using liposomes containing either cholesterol [^{14}C]oleate or the same type of liposomes containing [^{14}C]DPPC. The radioactivity in the cholesterol [^{14}C]oleate can now be expressed as a percentage of the radioactivity in [^{14}C]DPPC in a parallel incubation to monitor loss of cholesterol [^{14}C]oleate as a measure of hydrolysis.

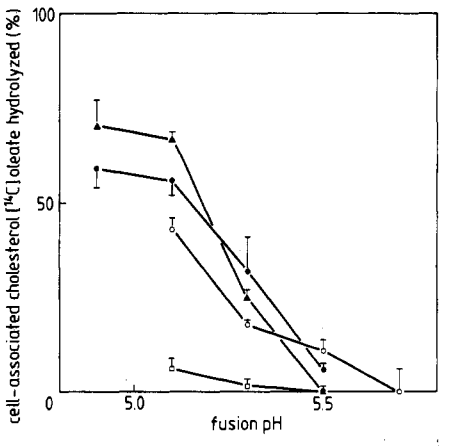

FIGURE 7: Induction of cholesterol ^{14}C-ester hydrolysis by low pH. A monolayer of MDCK cells in a 40-mm-diameter dish was infected with influenza N virus and treated with trypsin for 60 s at 37 °C, and liposomes containing cholesterol [^{14}C]oleate or [^{14}C]DPPC were bound and fused as in Figure 1. After being washed, the cell monolayer was left on ice covered with 1 mL of binding medium for 60 min and scraped from the dish. The individual data points represent the amount of cholesterol [^{14}C]oleate hydrolyzed as the percent of the [^{14}C]DPPC radioactivity present in a parallel incubation (see text). The bar indicates the SD (n = 4). (□) Small egg PC liposomes; (○) small egg PC/egg PE liposomes; (●) large egg PC/egg PE liposomes; (▲) large egg PC/soy PE liposomes.

A time course of cholesterol [^{14}C]oleate hydrolysis at 0 °C in the cell monolayer, after 60 s at pH 5.1, showed that the hydrolysis reaction was virtually completed in 30 min (results not shown). Further incubation at 0 °C or even an incubation of 10 min at 37 °C did not increase the level of hydrolysis. In contrast, after fusion of egg PC, egg PC/saturated PE, and egg PC/egg PE liposomes with MDCK cells, hydrolysis did not reach a plateau in 60 min at 0 °C, and incubation for at least 120 s at 37 °C in pH 7.4 medium was needed after the low-pH incubation. [^{14}C]DPPC was completely resistant to hydrolysis for at least 10 min at 37 °C after the low-pH step.

The pH dependence of the induction of cholesterol [^{14}C]-oleate hydrolysis is shown in Figure 7. Cholesterol [^{14}C]oleate becomes available for hydrolysis after a pH 5.5 incubation at 37 °C, and the amount of cholesterol [^{14}C]oleate available for hydrolysis reaches a maximum at pH 5.1. This pH dependence is identical with that displayed by the induction of neuraminidase-resistant binding (Figure 1) and that of the induction of loss of energy transfer (Figure 3). The time course with which the cholesterol [^{14}C]oleate becomes available for hydrolysis is shown in Figure 8. A striking similarity again exists between these time courses and those of the loss of energy transfer (Figure 4). The levels of hydrolysis, however, are somewhat lower than those of the loss of energy transfer. Like the loss of resonance energy transfer, the process is highly stimulated by the incorporation of unsaturated PE's into the liposomes and far less by a saturated PE. These similarities to the loss of resonance energy transfer strongly suggest that the cholesterol [^{14}C]oleate only becomes available for hydrolysis when the liposome has fused with the plasma membrane of the cell.

Low-pH-induced hydrolysis of cholesterol [^{14}C]oleate was also observed in BHK cells and in a different strain of MDCK cells, strain I [for nomenclature, see Balcarova-Ständer et al. (1984) and Fuller et al. (1984)]. When large egg PC/egg PE liposomes were fused with BHK cells for 60 s at pH 5.1, 73% ± 6% (n = 2) of the cholesterol [^{14}C]oleate was hydrolyzed during a subsequent 30-min incubation at 0 °C (cf. Figure 5). For MDCK strain I cells, the corresponding number was 70% ± 4% (n = 2). In neither cell line was the cholesterol

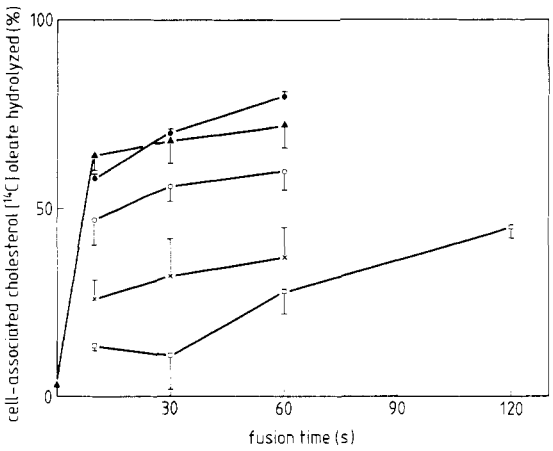

FIGURE 8: Time course of the induction of cholesterol [^{14}C]oleate hydrolysis by pH 5.1. In parallel incubations, liposomes with either cholesterol [^{14}C]oleate or [^{14}C]DPPC were bound to virus-infected, trypsin-treated MDCK cells and fused at pH 5.1 as in Figure 7. After various times at 37 °C and pH 5.1, the cell monolayer was washed 3 times with ice-cold binding medium and warmed to 37 °C at pH 7.4 for an additional period of 2 min. Subsequently, the cells were left on ice with 1 mL of PBS for 30 min, after which they were scraped from the dish and extracted. The lipids were analyzed as described under Materials and Methods, and the results were plotted as in Figure 7. The bar indicates the SD (n = 4). (□) Small egg PC liposomes; (○) small egg PC/egg PE liposomes; (●) large egg PC/egg PE liposomes; (×) large egg PC/saturated PE liposomes; (▲) large egg PC/soy PE liposomes.

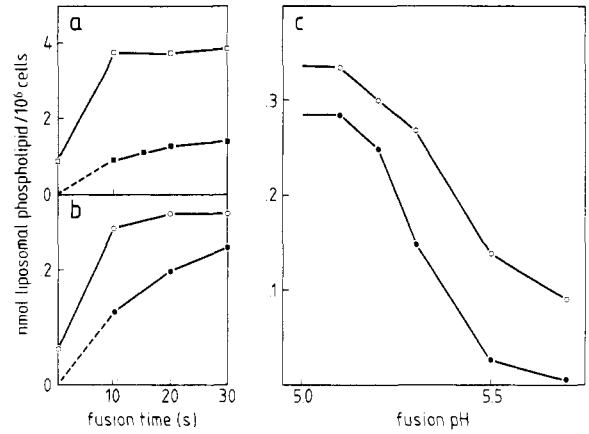

FIGURE 9: Comparison between absolute amounts of neuraminidase-resistant liposome–cell association and loss of resonance energy transfer upon fusion with MDCK cells. The data on the induction of neuraminidase resistance (open symbols) were taken from Figures 1 and 2, and the absolute amounts of liposomes fused according to loss of energy transfer (closed symbols) were calculated from Figures 2 and 4 for panels a and b and from Figures 1 and 3 for panel c. (a) Small egg PC liposomes; (b) small egg PC/egg PE liposomes; (c) large egg PC/egg PE liposomes.

[^{14}C]oleate hydrolyzed when the cells were incubated at pH 7.4 instead of at pH 5.1. [^{14}C]DPPC was resistant against hydrolysis in both cell lines, also after fusion. A different fate of the released fatty acids was obserbed in MDCK and BHK cells. Whereas esterification into phospholipids took place immediately in MDCK strain I cells ($t_{1/2}$ < 5 min at 0 °C), this process was much slower ($t_{1/2}$ ~ 60 min) in MDCK strain II cells with an intermediate rate for BHK cells.

In addition to cholesterol [^{14}C]oleate, nonexchangeable glycerol tri[^{14}C]oleate (Zilversmit, 1971) was used as a liposome marker. The behavior of this triglyceride when fused with BHK cells, MDCK strain I cells, or MDCK strain II cells was virtually identical with that of the cholesterol ester: after fusion at pH 5.1, glycerol tri[^{14}C]oleate became available for hydrolysis, while it was completely stable after incubation at pH 7.4.

Discussion

Previous studies of introducing exogenous lipids into the plasma membrane of living cells have had to make use of lipids which exchange spontaneously through the aqueous phase. Satisfactory methods have not been available which would allow controlled fusion of liposomes directly into the cell surface membrane. Some interesting results have been obtained by the use of this class of probes [see Dragsten et al. (1981), Pagano (1983), and Sleight & Pagano (1984)]. However, to study traffic of lipids in animal cells, it is necessary to use lipid molecules which as much as possible mimic the natural lipids in cellular membranes. We have designed a method which makes it possible to fuse lipid molecules at will by low pH into the plasma membrane of influenza virus infected cells. We have in this paper employed various critical assays to characterize the liposome–plasma membrane fusion process in more detail.

Sequential Stages in the Fusion Process. The neuraminidase-resistance assay indicated a rapid pH-dependent change in the type of binding of liposomes to the plasma membrane. This change was not correlated with positive evidence for fusion from the loss of resonance energy transfer, the cholesterol ester hydrolysis, or the lateral diffusion measurements. Our findings suggest, therefore, that the fusion reaction induced by low pH occurs in two separable stages. In the first stage, a change takes place in the binding of the liposome to the plasma membrane, from sialic acid mediated to a form where either sialic acid is no longer accessible to neuraminidase or it is no longer involved in binding. This stage precedes the actual liposome–plasma membrane fusion as monitored by all other fusion assays we have used (Figure 9). An additional difference between the conversion in liposome–plasma membrane binding and the actual fusion is that only the actual fusion is dependent on the liposomal lipid composition (Figure 2). The change in the type of binding has to be considered as a part of the fusion process since, in contrast to the inltial sialic acid mediated binding, it is strictly dependent both on the cleavage of HA into its fusogenic HA_1 and HA_2 subunits and on low pH (van Meer & Simons, 1983).

A change in the type of binding as an initial step in HA-mediated fusion has been suggested before (Gething et al., 1978; Skehel et al., 1982). At low pH, a conformational change occurs in the HA glycoprotein whereby HA_2, the subunit of the spike that is anchored in the viral membrane, exposes a second hydrophobic peptide segment [for a review, see White et al. (1983)] which is assumed to penetrate into the target membrane. As a consequence, the two apposed membranes would become linked by the HA protein, forming a bridge which is anchored in both membranes by hydrophobic peptide segments before actual fusion of the bilayer occurs. This model is supported by the observation that low pH induces binding of the bromelain fragment of HA to liposomes (Skehel et al., 1982), and by recent findings which show that the HA_2 subunit is responsible for this behavior and that the binding is not dependent on the liposomal lipid composition (Doms et al., 1985).

Both steps of the fusion process are highly dependent on pH (Figures 1, 3, and 7). In Figure 9, the net amount of lipid that has fused at any given pH is shown. Fusion takes place at pH <5.5 and reaches a maximum at pH 5.1. Identical curves were found for MDCK and BHK cells. This pH dependence agrees well with that reported for the induction of cell–cell fusion by intact influenza N virus (Huang et al.,

1981). The shape of the curve also fits well with the pH dependence of fowl plague virus, another avian influenza A virus strain (White et al., 1982, 1983), although in general the pH dependence of fusion for other influenza A viruses seems to be steeper (Maeda et al., 1981; White et al., 1983). The rates of HA-mediated liposome–cell fusion (Figure 4) are in the same range as those reported for the fusion of liposomes with intact influenza virus (Maeda et al., 1981; White et al., 1982).

Lipid Composition Dependence of the Fusion Process. For PE-containing liposomes, the pH dependence is much sharper than for PC liposomes (Figure 9). The reason for this difference, which lies in the second step of the fusion reaction (Figure 3), is not clear at this moment. Also, the level of fusion reached after 60 s at a certain pH was highly dependent on the liposome lipid composition. This is due to a difference in the rates of fusion. Liposomes containing PE with a high degree of unsaturation fuse 2 times faster than PC liposomes, while a virtually saturated PE has only little effect. A stimulating effect of the highly unsaturated soy PE has also been reported for the fusion of liposomes to intact influenza virus (White et al., 1982). Enhanced rates of fusion upon replacement of PC by PE have been reported in recent years for a variety of model membrane systems. The reason for this effect may be found in two properties of PE's: First, PE reduces the respulsive hydration force between bilayers (Lis et al., 1982), and second, PE, especially the more unsaturated species, exhibits a tendency to assume nonbilayer configurations (Cullis & de Kruyff, 1978) which have been suggested to be intermediate structures in the fusion reaction.

We also tested the effect of including PS in the liposomes. In model membrane systems, PS displays a strong fusogenic activity. This activity is induced by Ca^{2+} [see Papahadjopoulos (1979)]. In the present study, PS, apart from causing higher (nonspecific) binding, did not stimulate the actual fusion. Low-pH-induced liposome–plasma membrane fusion is not dependent on Ca^{2+} (van Meer & Simons, 1983).

Cell Type Dependence of the Fusion Process. Cell type had a strong influence on the fusion rates observed. Fusion with the plasma membrane of BHK cells was faster than fusion with MDCK cells. This is probably due to the fact that the apical plasma membrane domain of MDCK cells, with which the liposomes fuse, is a highly specialized part of the plasma membrane. Its protein and lipid composition differ from the rest of the plasma membrane [see Rodriguez-Boulan (1983) and van Meer & Simons (1982)], and in analogy with two different types of epithelial cells, Madin–Darby bovine kidney cells (Klenk & Choppin, 1970) and intestinal cells (Kawai et al., 1974), 50% of the lipids in this membrane domain may consist of glycolipids. Since glycolipids have been localized exclusively in the extracytoplasmic monolayer of the plasma membrane of mammalian cells (Gahmberg & Hakomori, 1973; Steck & Dawson, 1974; Stoffel et al., 1975; Stoffel & Sorgo, 1976), this leaflet of the apical membrane in epithelial cells may be greatly enriched in glycolipids. In contrast, BHK cells have only 5–10% glycolipids in their plasma membrane (Klenk & Choppin, 1970; Renkonen et al., 1972). This difference in lipid composition may be the reason for the different fusion rates observed with the two cell lines.

Cholesterol Oleate and Triacylglycerol Hydrolysis after Fusion. In the course of this study, we noticed that when cholesterol [^{14}C]oleate was included as a liposome label, the amount of liposomes which was found cell associated after low-pH fusion appeared much lower than when [^{14}C]DPPC was used to label the liposomes. This discrepancy was found to be due to hydrolysis of cholesterol oleate by a cellular hydrolase, presumably present in the plasma membrane of MDCK and BHK cells. The pH dependence, time course, and lipid dependence of cholesterol oleate hydrolysis correlated well with those measured by loss of resonance energy transfer after liposome fusion, arguing that cholesterol oleate hydrolysis can be used as a fusion assay to monitor liposome fusion in these cells. When glycerol trioleate was included into liposomes instead of cholesterol oleate, it was also hydrolyzed after low-pH fusion. The identity of the enzyme(s) responsible for both of these activities is not known. That the hydrolysis took place in the lysosomes is highly unlikely since this would imply that up to 60% of the cholesterol [^{14}C]oleate had been endocytosed and transported to the lysosome within 10 s at 37 °C. Apart from lysosomal hydrolases, different cholesterol esterases have been found in the plasma membrane and cytoplasm of several cells (Eto & Suzuki, 1973; Riddle et al., 1975; Nilsson, 1976). Furthermore, some of these cholesterol esterases have been reported to be identical with or complexed to a triacylglycerol lipase (Teng & Kaplan, 1974; Pittman & Steinberg, 1977; Cook et al., 1982; Blaner et al., 1984). The fact that newly inserted cholesterol oleate or triglyceride is quantitatively hydrolyzed predicts that neither of these lipids is normally present in plasma membranes.

Local and Long-Range Diffusion after Fusion. The combined study of various nonexchangeable lipids such as the fluorescent head-group derivatives of PE (Struck et al., 1981), the radioactive cholesterol ester (Kamp et al., 1973; Rothman & Dawidowicz, 1975), and triacylglycerol (Zilversmit, 1971) has proven its value in this study describing the interactions between liposomes and the plasma membrane lipid bilayer. We followed the fate of these nonexchangeable lipid molecules after fusion of liposomes with the plasma membrane. First, there is a local dilution of the lipid probes on a rapid time scale as determined by the loss of resonance energy transfer. Second, long-range lateral diffusion could be detected, and this shows that the water-insoluble fluorescent phospholipids are incorporated into a large, continuous membrane domain which from its size must be the plasma membrane. Third, the fused lipids became accessible to cellular hydrolase(s), which degrade(s) cholesterol esters and triglycerides. On the basis of these findings, we are confident that application of this implantation method to a variety of (natural) lipids in combination with the construction of asymmetric liposomes should provide useful tools to study lipid transport and metabolism in mammalian cells.

ACKNOWLEDGMENTS

We thank Doris Hübsch and Hilkka Virta for excellent technical assistance, Annie Steiner for typing the manuscript, and Petra Riedinger for preparing the drawings. We are grateful to Barry Gumbiner and Graham Warren for critically reading the manuscript.

Registry No. *N*-Rh-PE, 78346-67-5; *N*-NBD-PE, 91632-07-4; cholesterol, 57-88-5; neuraminidase, 9001-67-6; cholesterol oleate, 303-43-5; octyl β-D-glucoside, 29836-26-8.

REFERENCES

Balcarova-Ständer, J., Pfeiffer, S. E., Fuller, S. D., & Simons, K. (1984) *EMBO J. 3*, 2687–2694.

Bental, M., Lelkes, P. I., Scholma, J., Hoekstra, D., & Wilschut, J. (1984) *Biochim. Biophys. Acta 774*, 296–300.

Blaner, W. S., Prystowsky, J. H., Smith, J. E., & Goodman, D. S. (1984) *Biochim. Biophys. Acta 794*, 419–427.

Bligh, E. G., & Dyer, W. J. (1959) *Can. J. Biochem. Physiol. 37*, 911–917.

Cook, K. G., Yeaman, S. J., Stralfors, P., Fredrikson, G., & Belfrage, P. (1982) *Eur. J. Biochem. 125*, 245–249.
Crawford, C. G., & Plattner, R. D. (1984) *J. Lipid Res. 25*, 518–522.
Cullis, P. R., & de Kruyff, B. (1978) *Biochim. Biophys. Acta 513*, 31–42.
Davoust, J., Devaux, P. F., & Leger, L. (1982) *EMBO J. 1*, 1233–1238.
Doms, R. W., Helenius, A., & White, J. (1985) *J. Biol. Chem. 260*, 2973–2981.
Dragsten, P. R., Blumenthal, R., & Handler, J. S. (1981) *Nature (London) 294*, 718–722.
Eidelman, O., Schlegel, R., Tralka, T. S., & Blumenthal, R. (1984) *J. Biol. Chem. 259*, 4622–4628.
Ekerdt, R., Dahl, G., & Gratzl, M. (1981) *Biochim. Biophys. Acta 646*, 10–22.
Eto, Y., & Suzuki, K. (1973) *J. Biol. Chem. 248*, 1986–1991.
Fuller, S., von Bonsdorff, C.-H., & Simons, K. (1984) *Cell (Cambridge, Mass.) 38*, 65–77.
Fung, B. K.-K., & Stryer, L. (1978) *Biochemistry 17*, 5241–5248.
Gahmberg, C. G., & Hakomori, S. (1973) *J. Biol. Chem. 248*, 4311–4317.
Gething, M. J., White, J. M., & Waterfield, M. D. (1978) *Proc. Natl. Acad. Sci. U.S.A. 75*, 2737–2740.
Gregoriadis, G. (1980) in *Liposomes in Biological Systems* (Gregoriadis, G., & Allison, A. C., Eds.) pp 25–86, Wiley, New York.
Helenius, A., Fries, E., & Kartenbeck, J. (1977) *J. Cell Biol. 75*, 866–880.
Helenius, A., Sarvas, M., & Simons, K. (1981) *Eur. J. Biochem. 116*, 27–35.
Holub, B. J., & Kuksis, A. (1969) *Lipids 4*, 466–472.
Huang, R. T. C., Rott, R., & Klenk, H.-D. (1981) *Virology 110*, 243–247.
Jagannatha, H. M., & Sastry, P. S. (1981) *J. Neurochem. 36*, 1352–1360.
Kamp, H. H., Wirtz, K. W. A., & van Deenen, L. L. M. (1973) *Biochim. Biophys. Acta 318*, 313–325.
Kawai, K., Fujita, M., & Nakao, M. (1974) *Biochim. Biophys. Acta 369*, 222–233.
Klein, R. A. (1970) *Biochim. Biophys. Acta 210*, 486–489.
Klenk, H.-D., & Choppin, P. W. (1970) *Proc. Natl. Acad. Sci. U.S.A. 66*, 57–64.
Klenk, H.-D., Rott, R., Orlich, M., & Blödorn, J. (1975) *Virology 68*, 426–439.
Lanni, F., & Ware, B. R. (1984) *Biophys. J. 46*, 97–110.
Lis, L. J., McAlister, M., Fuller, N., Rand, R. P., & Parsegian, V. A. (1982) *Biophys. J. 37*, 657–666.
Maeda, T., Kawasaki, K., & Ohnishi, S.-I. (1981) *Proc. Natl. Acad. Sci. U.S.A. 78*, 4133–4137.
Matlin, K. S., & Simons, K. (1983) *Cell (Cambridge, Mass.) 34*, 233–243.
Matlin, K. S., Reggio, H., Helenius, A., & Simons, K. (1981) *J. Cell Biol. 91*, 601–613.
Miles, D. G., Primakoff, P., & Koppel, D. E. (1984) *J. Cell Biol. 98*, 1905–1909.
Nilsson, A. (1976) *Biochim. Biophys. Acta 450*, 379–389.
Pagano, R. E. (1983) in *Liposome Letters* (Bangham, A. D., Ed.) pp 83–95, Academic Press, New York.
Papahadjopoulos, D., Poste, G., & Vail, W. J. (1979) *Methods Membr. Biol. 10*, 1–121.
Pittman, R. C., & Steinberg, D. (1977) *Biochim. Biophys. Acta 487*, 431–444.
Renkonen, O., Gahmberg, C. G., Simons, K., & Kääriäinen, L. (1972) *Biochim. Biophys. Acta 255*, 66–78.
Riddle, M. C., Smuckler, E. A., & Glomset, J. A. (1975) *Biochim. Biophys. Acta 388*, 339–348.
Rodriguez-Boulan, E. (1983) *Mod. Cell Biol. 1*, 119–170.
Rogers, G. N., Paulson, J. C., Daniels, R. S., Skehel, J. J., Wilson, I. A., & Wiley, D. C. (1983) *Nature (London) 304*, 76–78.
Rothman, J. E., & Dawidowicz, E. A. (1975) *Biochemistry 14*, 2809–2816.
Rouser, G., Fleischer, S., & Yamamoto, A. (1970) *Lipids 5*, 494–496.
Schneider, H., Lemasters, J. J., Höchli, M., & Hackenbrock, C. R. (1980) *Proc. Natl. Acad. Sci. U.S.A. 77*, 442–446.
Skehel, J. J., Bayley, P. M., Brown, E. B., Martin, S. R., Waterfield, M. D., White, J. M., Wilson, I. A., & Wiley, D. C. (1982) *Proc. Natl. Acad. Sci. U.S.A. 79*, 968–972.
Sleight, R. G., & Pagano, R. E. (1984) *J. Cell Biol. 99*, 742–751.
Smith, B. A., & McConnell, H. M. (1978) *Proc. Natl. Acad. Sci. U.S.A. 75*, 2759–2763.
Smith, B. A., Clark, W. R., & McConnell, H. M. (1979) *Proc. Natl. Acad. Sci. U.S.A. 76*, 5641–5644.
Steck, T. L., & Dawson, G. (1974) *J. Biol. Chem. 249*, 2135–2142.
Stoffel, W., & Sorgo, W. (1976) *Chem. Phys. Lipids 17*, 324–335.
Stoffel, W., Anderson, R., & Stahl, J. (1975) *Hoppe-Seyler's Z. Physiol. Chem. 356*, 1123–1129.
Struck, D. K., Hoekstra, D., & Pagano, R. E. (1981) *Biochemistry 20*, 4093–4099.
Teng, M.-H., & Kaplan, A. (1974) *J. Biol. Chem. 249*, 1064–1070.
van Meer, G., & Simons, K. (1982) *EMBO J. 1*, 847–852.
van Meer, G., & Simons, K. (1983) *J. Cell Biol. 97*, 1365–1374.
White, J., Kartenbeck, J., & Helenius, A. (1982) *EMBO J. 1*, 217–222.
White, J., Kielian, M., & Helenius, A. (1983) *Q. Rev. Biophys. 16*, 151–195.
Zilversmit, D. B. (1971) *J. Biol. Chem. 246*, 2645–2649.